13th World Conference on Earthquake Engineering
Vancouver, B.C., Canada
August 1-6, 2004
Paper No. 664

PSEUDO NEGATIVE STIFFNESS DAMPERS FOR EARTHQUAKE RESPONSE CONTROL OF CABLE-STAYED BRIDGES

Hirokazu IEMURA[1] and Mulyo Harris PRADONO[2]

SUMMARY

Seismic response control of cable-stayed bridge discussed herein is to provide special bearings at the deck-tower connections to reduce the seismic induced force and displacement. Elastic bearings plus special dampers are employed as the control devices.

The dampers are the newly proposed pseudo-negative-stiffness-controlled damper. Practical advantage is that control algorithm is simple and sensors are required only at the damper to measure relative displacement and velocity. The system has been verified experimentally in the laboratory.

The control algorithm commands the variable damper to produce pseudo negative stiffness hysteretic loop. That is, unlike linear viscous damper that produces elliptical shape hysteretic loop, the controlled variable damper produces hysteretic loop that represent combination of negative stiffness and viscous damping.

The point is that the combination of pseudo negative stiffness hysteretic loop plus elastic bearing stiffness produces artificial hysteretic loop that approaches rigid-perfectly plastic force-deformation characteristics which has large damping ratio.

In order to study the effectiveness of this damper for seismic response control of cable-stayed bridges, application of pseudo negative stiffness damper and linear viscous damper to a typical cable-stayed bridge in Japan and to the benchmark cable-stayed bridge in the US was carried out using numerical simulations under several earthquake excitations. The results show that the pseudo negative stiffness damper reduces seismic responses better than those by passively viscous damper.

INTRODUCTION

[1] Professor, Structural Dynamics Laboratory, Urban Management Department, Kyoto University, Sakyo-ku, Kyoto 606-8501, Japan. E-mail: iemura@catfish.kuciv.kyoto-u.ac.jp
[2] Post-doctoral Fellow, Structural Dynamics Laboratory, Urban Management Department, Kyoto University, Sakyo-ku, Kyoto 606-8501, Japan. E-mail: pradono@catfish.kuciv.kyoto-u.ac.jp

Cable-stayed bridges are very appealing aesthetically and very important lifeline structures. The increasing popularity of these bridges among bridge engineers can be attributed to the appealing aesthetics, full and efficient utilization of structural materials, increased stiffness over suspension bridges, efficient and fast mode of construction, and relatively small size of substructure.

However, from the structural dynamics point of view, cable-stayed bridges exhibit complex behavior in which the vertical, lateral, and torsional motions are often strongly coupled (Dyke et al. [1]). These flexible structures raise many concerns about their behavior under environmental dynamic loads such as wind and earthquake.

From the analyses of various observational data, including ambient and forced vibration tests of cable-stayed bridges, it is known that these bridges have very small mechanical or structural damping (0.3 – 2.0%) (Abdel-Ghaffar [2]). The fact that cable-stayed bridges possess little damping characteristics to help alleviate vibration under severe ground motions, wind turbulence, and traffic loadings spurred recent efforts to enhance the technology of structural control, whether it is active, passive, semi-active or combination thereof to alleviate dynamic responses.

The merit of active control is that they are effective for wide-frequency range. However, the active control needs a large amount of external energy supply that is not always available during strong earthquake attack and also high level of maintenance.

On the other hand, Spencer and Sain [3] claimed that many active control for systems for civil engineering applications operate primarily to modify structural damping. Their preliminary studies indicate that appropriately implemented semi-active systems perform significantly better than passive devices and have the potential to achieve the majority of the performance of fully active systems, thus allowing for the possibility of effective response reduction during a wide array of dynamic loading conditions, without requiring the associated large power sources.

Moreover, a semi-active control device is one which cannot inject mechanical energy into the controlled structure system, therefore, in contrast to active control devices, semi-active control devices do not have the potential to destabilize (in the bounded input/ bounded output sense) the structural system. Control strategies based on semi-active devices appear to give a promising future as the devices combine the best feature of both active and passive control systems. Therefore this strategies have recently been widely investigated to reduce the dynamic response of structures subjected to earthquake and wind excitations.

PSEUDO NEGATIVE STIFFNESS CONTROLLED DAMPERS

Commonly semi-active strategies still use active control algorithm for primary controller (e.g., Dyke et al. [4], Jung et al. [5]), so that the number of sensors are the same as those for active control, plus additional force sensors to make the actual force track the desired force commanded by the primary controller.

Moreover, as the whole system is an integrated system controlled by single controller, malfunction of this controller will be disadvantageous to the whole structural system.

As an attempt to overcome these problems, another type of semi-active control that uses less sensors and much simpler control algorithm has been proposed by Iemura et al. [6] and Iemura and Pradono [7]. The algorithm can controls each damper independently, therefore, in case of one controller should malfunction, it does not affect the performance of other devices.

The strategy is to create pseudo negative stiffness hysteretic loop produced by a variable damper. The variable damper that can produce this kind of hysteretic loop is then called herein "pseudo negative stiffness (PNS) damper".

The point is that damper is usually set parallel to existing member that has some stiffness. Viscous dampers, for example, have elliptical hysteretic loops (**Figure 1b**) when excited by sinusoidal excitations. Since the force transferred to other members is the summation of the damper and existing-member stiffness forces, then it is interesting to see **Figure 1c**, which is the summation of existing-member stiffness force and damper force. It is clear that the maximum forces in **Figure 1c** is larger the maximum existing-member forces in **Figure 1a**.

On the other hand, by producing pseudo negative stiffness (PNS) hysteretic loops (**Figure 1e**), the maximum forces in **Figure 1f** is kept the same with existing-member stiffness forces (**Figure 1d**) while keeping large area inside the hysteretic loops.

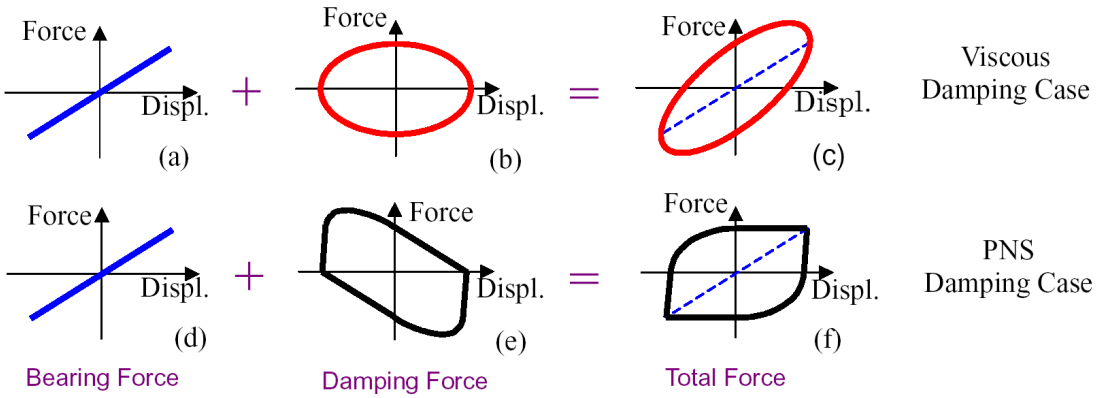

Figure 1 Total Force at Bearing Location

Experimental test has been performed by Iemura et al. [6] on a variable orifice oil damper (**Figure 2**). From the experiment results, the damping force F available for this damper is shown in **Equation (1)**. Where $\dot{u}$ is piston velocity, sgn($\dot{u}$) is piston direction, and h is the valve opening ratio.

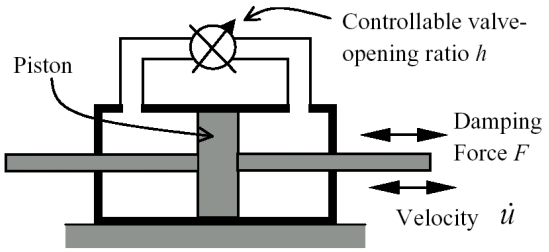

Figure 2 Schematic of Variable Orifice Oil Damper

$$F = \mathrm{sgn}(\dot{u})\left[\left(\frac{159.23}{h^2} + 307.2\right)\dot{u}^2 + 0.6\right](\mathrm{kN}) \qquad (1)$$

Force demand for this damper is shown in **Equation (2)**, which is called herein PNS control law. F_d is the force demand, K_d is a selected negative stiffness value, C_d is a selected damping coefficient, and u is piston displacement (stroke). The discussion about the values of K_d and C_d can be found in the work by the authors (Iemura and Pradono [8]).

$$F_d = K_d u + C_d \dot{u} \tag{2}$$

The variable damper force F must be kept as near as possible to the force demand F_d. This can be done by adjusting valve opening ratio h at every time step depending upon the velocity $\dot{u}$ on that step.

The opening ratio h can be calculated by substituting **Equation (2)** into **Equation (1)** as shown in **Equation (3)**. The equation has a meaning that when the direction of the demanded force is opposed to the velocity direction, the opening ratio is chosen for the variable damper to generate as small force as possible. For information, the opening ratio h can only be adjusted from $h_{\min} = 0.05$ to $h_{\max} = 0.80$ for this kind of damper.

$$h = \sqrt{\frac{159.232}{\frac{\left(\frac{F_d}{\mathrm{sgn}(\dot{u})} - 0.6\right)}{\dot{u}^2} - 307.2}} \tag{3}$$

Under sinusoidal excitation with frequency ω, the force demand F_d in **Equation (2)** would be as shown in **Figure 3**, and the experimental result of damper force F is shown in **Figure 4**.

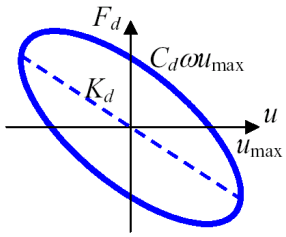

Figure 3 Force Demand

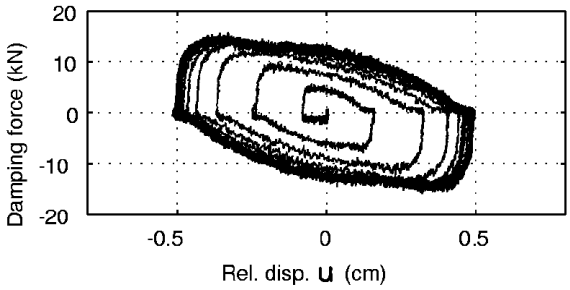

Figure 4 Hysteretic Loops, Experimental Result, Sinusoidal Excitation (1.8 Hz) (Iemura et al. [6])

The piston displacement, valve opening ratio, and Force-Velocity relationship are shown in **Figure 5**. The advantage of this method is that sensors are put only at the dampers to measure relative displacement and the controller can be made independently for each damper.

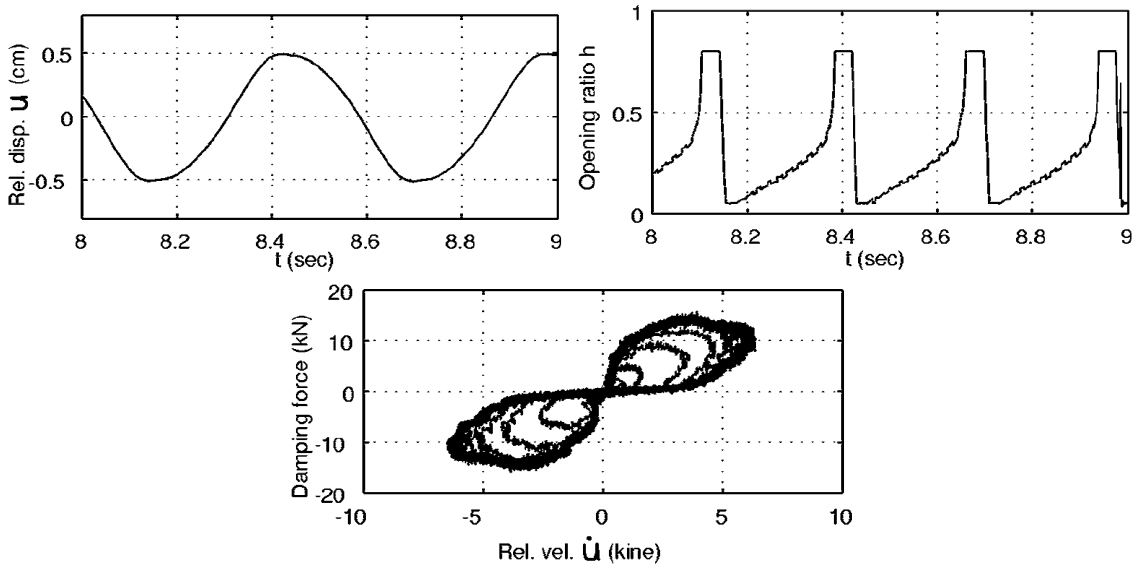

Figure 5 Piston Displacement, Valve Opening Ratio, and Force-Velocity Relationship for hysteretic loops shown in **Figure 4** (Iemura et al. [6])

APPLICATION OF PNS DAMPERS TO THE TEMPOZAN BRIDGE

Due to severe damages of many bridges caused by the Hyogo-ken Nanbu Earthquake in Kobe area in 1995, very high ground motion (level II design) is now required in the new bridge design specification set in 1996 (Japan Roadway Association [9]) in Japan, in addition to the relatively frequent earthquake motion (level I design) by which old structure were designed and constructed.

Hence, seismic safety of cable-stayed bridges, including the Tempozan Bridge, which were built before the present code specification has to be reviewed and seismic retrofit has to be done, if it is found necessary.

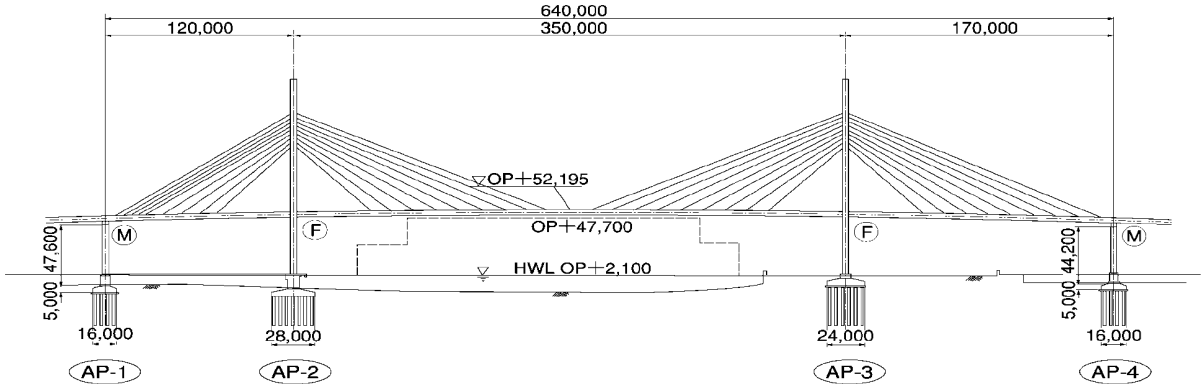

Figure 6 Drawing of the Tempozan Bridge (Side View)

The Tempozan Bridge

Tempozan Bridge, built in 1988, is a three-span continuous steel cable-stayed bridge which crosses the mouth of the Aji River, Osaka, Japan (Hanshin Highway Public Corporation [10]). The total length of the bridge is 640 m. (**Figure 6**). The cable in the superstructure is 2-plane fan pattern multi-cable system with 9 stay cables each plane. The main towers are A-shaped to have a good appearance and to improve the torsional rigidity.

The structure has fixed hinge connections (symbol **F** in **Figure 6**) between the deck and the tower. However, in the numerical model representing the Tempozan bridge, the fixed hinge connections are replaced with elastic bearings and PNS damper or viscous damper. The input ground acceleration used for study is Type I-III-1, I-III-2, and I-III-3 (artificial ground acceleration used for bridge design in Japan).

Basic Concept of Seismic Retrofit

The basic concept of retrofit by using structural control technology is to make the structure flexible and highly damped. This can be achieved by replacing the fixed-hinge connections between the deck and towers with flexible bearings so that the induced seismic forces will be kept to minimum values, and to add energy absorbing devices set parallel to the bearings to absorb large seismic energy and reduce the seismic response amplitudes (**Figure 7**). The energy absorbing devices studied herein are passive viscous damper and the pseudo negative stiffness (PNS) damper.

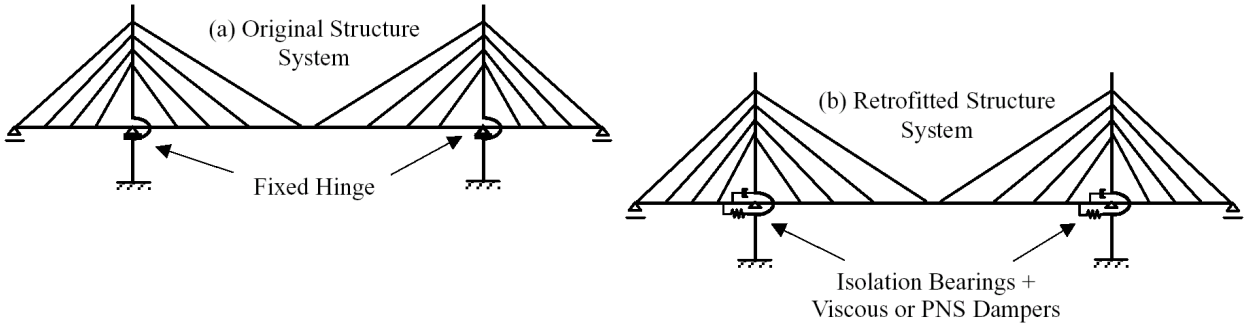

Figure 7 Retrofit System of a Cable-stayed Bridge

By replacing the fixed hinge connections between the deck and the tower with elastic bearings, modal shape analysis of the Tempozan bridge model shows lower curvature at the deck and the towers. The main natural period is also lengthened from 3.75 second to 6.31 second. More study about this matter and the bearing stiffness for this retrofit strategy can be found in other work by the authors (Iemura and Pradono [7]).

Numerical Simulations

The model of the bridge is then numerically simulated in which the damping force can be commanded based on PNS control algorithm. The simulation of the model with elastic bearings and PNS damper shows that under earthquake excitations, pseudo negative stiffness hysteretic loop was produced by the PNS damper (**Figure 8b**).

This hysteretic loop clearly differs from that of viscous damper (**Figure 8a**). Viscous damper here means K_d is set zero and C_d is optimized to produce the smallest base shear under design earthquakes. It produces structural damping ratio of 35.6% (Iemura and Pradono [7]). On the other hand, for the PNS damper, K_d is chosen as negative of the bearing stiffness, and C_d is the same with that of viscous damper.

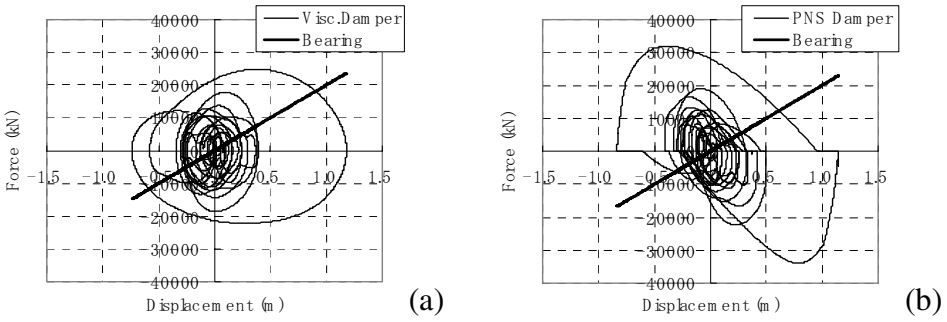

Figure 8 Damper and Bearing Force for (a) Viscous Damper case and (b) PNS Damper case

Since the force transferred to other members by damper and bearing is summation of damper and bearing force, it is interesting to see **Figure 9**, which shows the summation of the damper hysteretic loop in **Figure 8** with the bearing force.

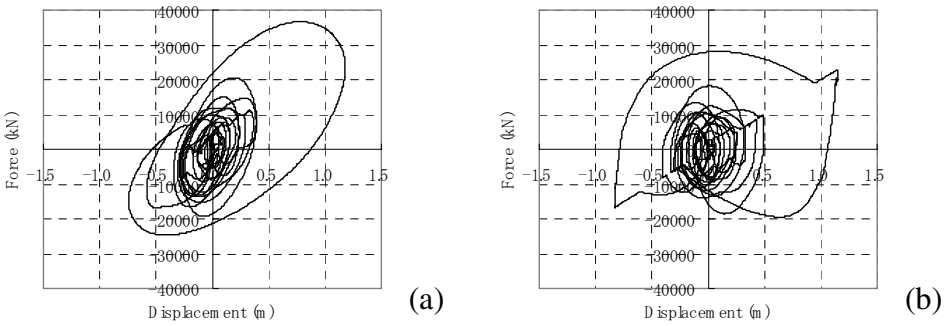

Figure 9 Damper + Bearing Force for (a) Viscous Damper case and (b) PNS Damper case

It is clear from the figure that combination of PNS damper force plus elastic bearing force results in lower force than that of viscous damper while keeping large area under hysteretic loop, which means large damping ratio. This is the main purpose of producing pseudo negative stiffness hysteretic loops.

Lower member forces will result in lower base shear, as it is shown in **Figure 10**, for longitudinal direction. This simulation shows the effectiveness of PNS damper in reducing both base shear and displacement of the cable-stayed bridge.

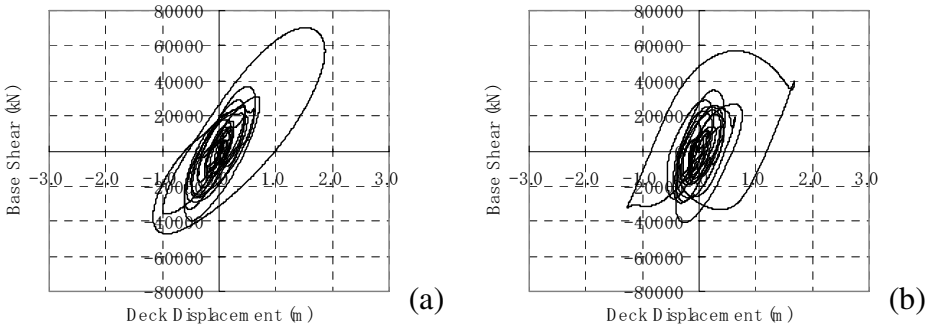

Figure 10 Base Shear Force for (a) Viscous Damper case and (b) PNS Damper case

APPLICATION OF PNS DAMPERS TO THE BENCHMARK CONTROL PROBLEM FOR CABLE-STAYED BRIDGES

It is generally impossible to compare different control strategies directly because the control methods were applied to different structures. This problem can be addressed by benchmark control problems for cable-stayed bridges. This will allow researchers to apply various control strategies, such as passive, active, semi-active, or combination thereof, to cable-stayed bridges, and to compare results directly in terms of a specified set of performance objectives (Dyke et al. [1]).

The benchmark control problems focus on Bill Emerson Memorial Bridge in Cape Girardeu, Missouri, USA. It is a cable-stayed bridge with total length of 636 meter, crossing the Mississippi river. The bridge is currently under construction and is expected to complete in 2003.

From the complete drawing of the bridge, three-dimensional finite element models were developed in MATLAB® (Mathworks [11]). The first model, serving as uncontrolled structure, has fixed hinge connections between the deck and the towers. Whereas the second model, shown in **Figure 11**, is serving as controlled structure. It has no connection between the deck and the tower to make it possible for researchers to add control devices. The natural periods of the controlled model are much longer than those of the uncontrolled model.

Benchmark Problem Statements

In the model, participants are to define the devices, sensors, and control algorithm used, and to evaluate the results in terms of specified evaluation criteria. There are eighteen evaluation criteria and each evaluation criterion is mainly a ratio between maximum responses of controlled and uncontrolled structures, except for the amount of devices and sensors.

The input ground motions are specified as (i) El Centro, recorded at the Imperial Valley Irrigation District substation in El Centro, California, May 18, 1940; (ii) Mexico, recorded at the Galeta de Campos station in September 19, 1985; and (iii) Gebze, The Kocaeli earthquake in Turkey recorded at the Gebze Tubitak Marmara Arastirma Merkezi on August 17, 1999. The earthquakes allow for the researcher to test his or her control strategies on earthquakes with different characteristics.

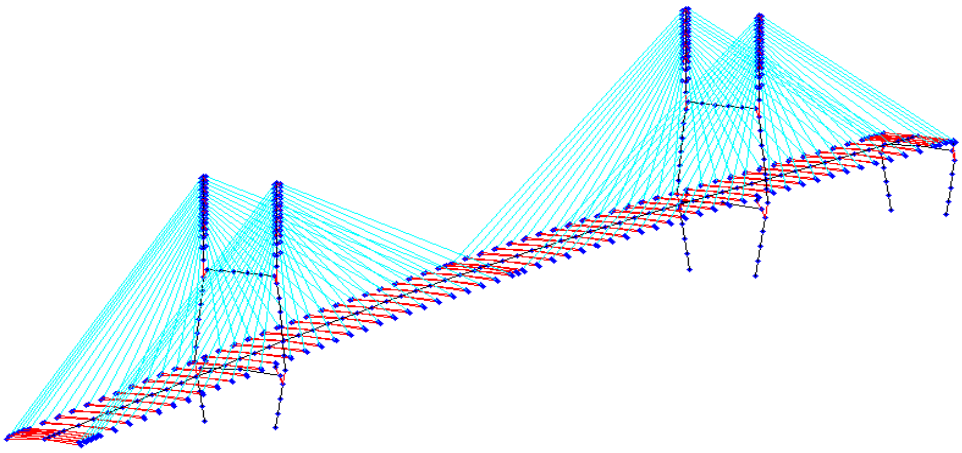

Figure 11 Finite Element Model of the Benchmark Control Problem for Cable-stayed Bridges

Application of the PNS Dampers

The application of PNS damper shown herein is for the first generation of benchmark problem. The application for the second generation is published elsewhere (Iemura and Pradono [8]).

Firstly, elastic bearings are applied between the deck and the towers of the controlled model, to provide stiffness needed to take back the deck to original position. Secondly, PNS or viscous dampers are applied parallel to the elastic bearing. For the viscous damper, K_d is set zero and C_d is optimized to produce the smallest base shear under the above three earthquakes. However, for the PNS damper, K_d is negative of the bearing stiffness and C_d is the same as that of the viscous damper.

Then, the controlled model with PNS damper (PNS case) and viscous damper (viscous case) is simulated under the three input earthquakes to obtain the results of the evaluation criteria.

The results of the evaluation criteria are shown in **Table 1**. The PNS case shows better results than the viscous case. Only the deviation of cable tension under El Centro earthquake is slightly unsatisfactory. The reason is that the PNS damper is set on a longitudinal direction of the bridge. On the other hand, the cable has vertical component that is not controllable by this longitudinal-direction damper.

Table 1. Results of the evaluation criteria

Evaluation Criteria	El Centro		Mexico		Gebze	
	Viscous	PNS	Viscous	PNS	Viscous	PNS
J_1 (shear force at tower base)	0.334	**0.327**	0.479	**0.448**	0.482	**0.467**
J_2 (shear force at deck level)	1.016	**0.933**	1.137	**1.047**	1.234	**1.193**
J_3 (moment at tower base)	0.300	**0.248**	0.607	**0.504**	0.532	**0.491**
J_4 (moment at deck level)	0.638	**0.516**	0.578	**0.536**	1.094	**0.890**
J_5 (deviation of cable tension)	**0.167**	0.175	0.063	**0.060**	0.123	**0.116**
J_6 (deck displacement)	1.340	**1.110**	2.511	**2.178**	2.798	**2.476**
J_7 (normed J_1)	0.227	**0.213**	0.405	**0.375**	0.412	**0.366**
J_8 (normed J_2)	0.989	**0.907**	1.015	**0.913**	1.220	**1.127**
J_9 (normed J_3)	0.297	**0.259**	0.513	**0.420**	0.567	**0.478**
J_{10} (normed J_4)	0.834	**0.761**	1.103	**0.955**	1.195	**1.066**
J_{11} (normed J_5)	0.024	**0.023**	0.009	**0.009**	0.016	**0.015**
J_{12} (force by control devices)	3.53e-3	**2.85e-3**	1.47e-3	**1.12e-3**	3.92e-3	**3.71e-3**
J_{13} (stroke of control devices)	0.876	**0.660**	0.404	**0.352**	1.449	**1.320**
J_{16} (no. of control devices)	**20**	**20**	**20**	**20**	**20**	**20**
J_{17} (number of sensors)	**0**	4	**0**	4	**0**	4

Note: - Number in **bold** shows better evaluation criteria
- "normed" means the comparison is done at every time step

The reason for almost all response for the PNS case is lower than the viscous case is fat hysteretic loop, low force, and small displacement as shown in the following figures.

Figure 12 shows the damper and the bearing hysteretic loops at one tower of the bridge. The damper and bearing hysteretic loops are shown in curved and straight lines, respectively. It is clear from the figure that PNS controlled dampers can produce pseudo negative stiffness hysteretic loops under the three different input earthquakes.

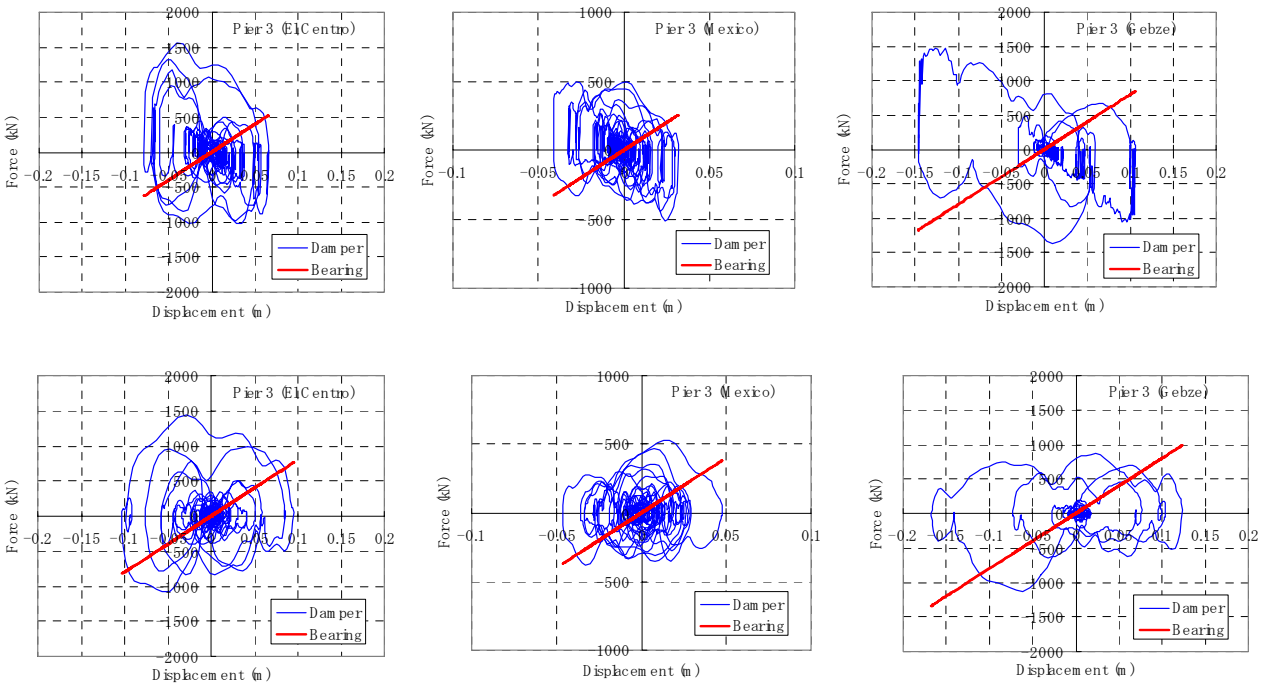

Figure 12 Damper and elastic bearing hysteretic loop for three earthquakes for (a) PNS damper and (b) Viscous damper

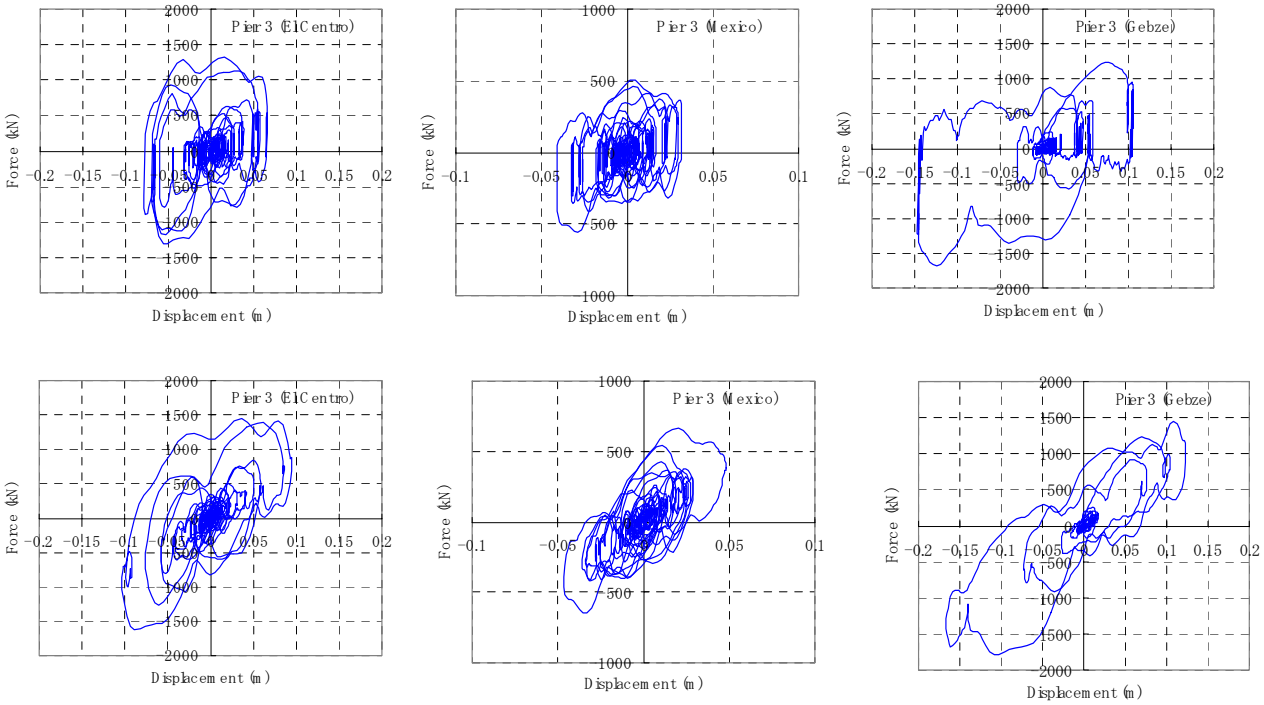

Figure 13 Damper + elastic bearing hysteretic loop for three earthquakes for (a) PNS damper and (b) Viscous damper

The total force of damper plus elastic bearing is shown in **Figure 13**. It is clear from the figure that PNS damper results in lower force and lower displacement than those of viscous damper, while keeping large energy absorption, because the hysteretic loop approaches that of rigid perfectly plastic force-deformation characteristics.

Earthquake Input Energy

The PNS damper is also effective in reducing the earthquake input energy in comparison with those of viscous damper as it is shown in **Figure 14**. The definition of the earthquake input energy used herein is represented by **Equation (4)**.

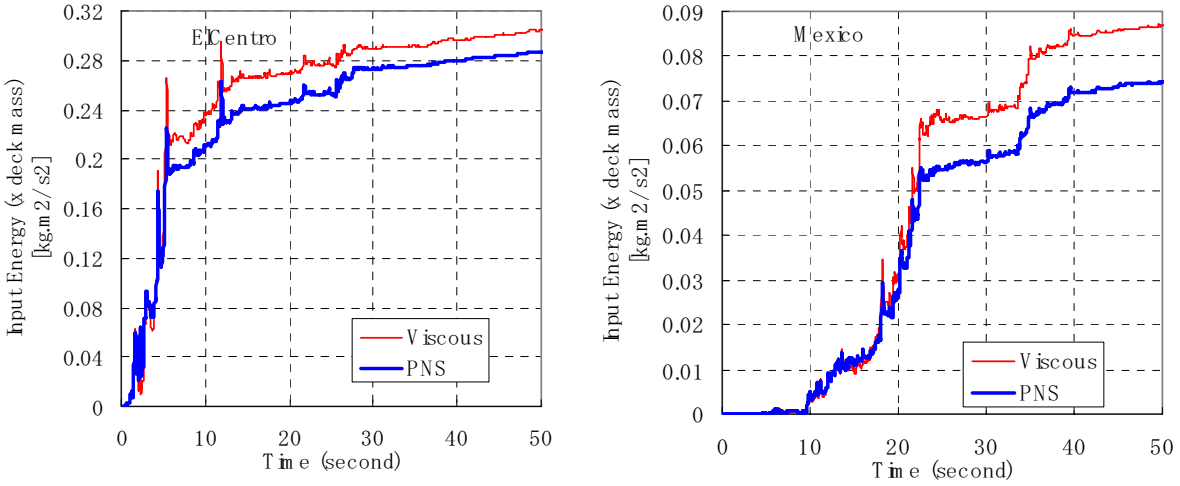

Figure 14. Earthquake input energy for both Viscous case and PNS case

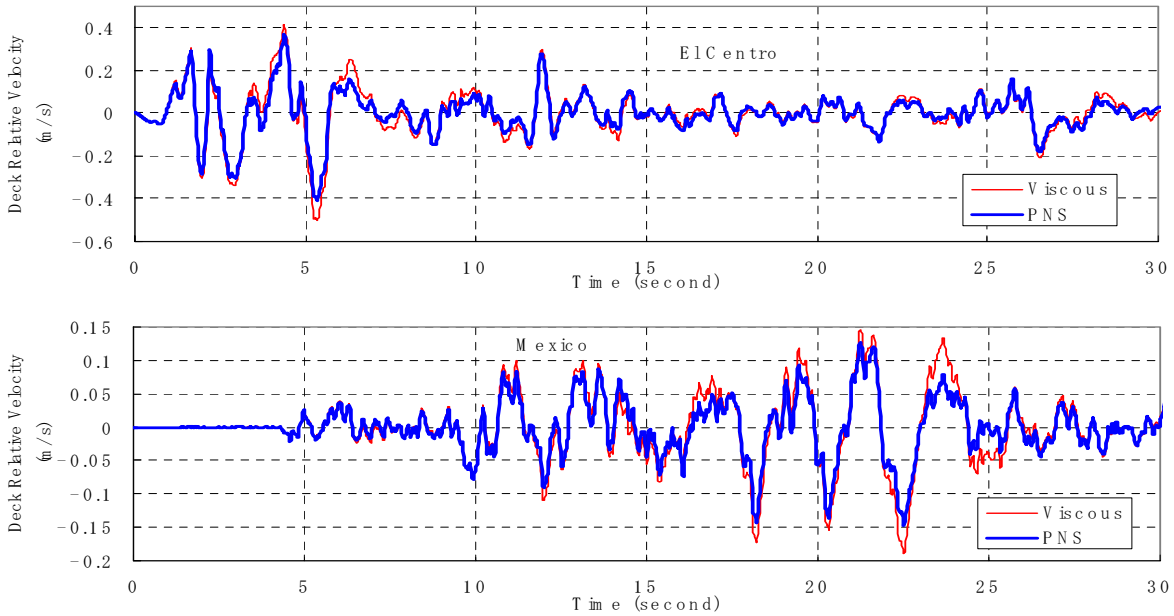

Figure 15. Deck relative velocity between PNS and viscous damper case for El Centro and Mexico earthquakes

The equation is a general definition for earthquake input energy (Chopra [12]), where E_I is the earthquake input energy and m_D is the deck mass. The ground acceleration is represented by $\ddot{z}_g$ and the deck velocity relative to the ground is represented by $\dot{u}_D$.

$$E_I = -\int_0^t m_D \ddot{z}_g \dot{u}_D dt \tag{4}$$

Since the deck velocity is lower for the PNS case (**Figure 15**), then the earthquake input energy is expected to be lower than that of the viscous case.

CONCLUSIONS

Numerical simulations on cable-stayed bridge models incorporating viscous damper and PNS damper have been carried out under earthquake excitations.

The viscous damping coefficient herein was optimized to produce the lowest base shear under design earthquakes. However, the viscous damper hysteretic loops combined with existing-member stiffness force produce forces that are significantly larger than the stiffness force.

On the other hand, the PNS damper hysteretic loop combined with existing-member stiffness force produce forces that are about the same with the stiffness force, because the combined hysteretic loop approaches that of artificially rigid perfectly-plastic force-deformation characteristics which have large damping ratio. So that the base shear and the displacement become lower than that of the optimized viscous damper above.

The earthquake input energy into the structure is also lower for cable-stayed bridge using PNS damper than that of linear viscous damper. It is because the deck velocity is lower for the PNS damper case.

REFERENCES

1. Dyke, S. J., Caicedo, J. M., Turan, G., Bergman, L. A., and Hague, S. Phase I Benchmark Control Problem for Seismic Response of Cable-stayed Bridges, *Journal of Structural Engineering*, Vol. 129, No. 7, pp. 857-872, July 1, 2003.
2. Abdel-Ghaffar, A. M. Cable-stayed bridges under seismic action. *Cable-stayed Bridges: Recent Developments and Their Future*, Editor: M. Ito, Elsevier Science Publishers, pp. 171-192, 1991.
3. Spencer, B. F. and Sain, M. K., Controlling Buildings: A New Frontier in Feedback, *Special Issue of the IEEE Control Systems Magazine on Emerging Technology*, Vol 17, No. 6, pp. 19-35, December 1997.
4. Dyke, S. J., Spencer, B F., Sain, M. K., and Carlson, J. D., Seismic Response Reduction using Magnetorheological Dampers, *Proc. IFAC World Congress*, San Francisco, California, 1996.
5. Jung, H-J, Spencer, B.F., Lee, I-W. Benchmark Control Problem for Seismically Excited Cable-stayed Bridges using Smart Damping Strategies. *Proc. IABSE Conference*, Session 7B, Seoul, June, 2001.
6. Iemura, H., Igarashi, A., and Nakata, N. Semi-active Control of Full-scale Structures using Variable Joint Damper System. *The 14th KKNN Symposium on Civil Engineering*, Kyoto, Japan, pp. 41-46, November 5-7, 2001.

7. Iemura, H. and Pradono, M. H., Passive and Semi-active Seismic Response Control of a Cable-stayed Bridge, *Journal of Structural Control*, John Wiley and Sons, Vol. 9, pp. 189-204, December, 2002.
8. Iemura, H. and Pradono, M. H., Application of Pseudo-negative Stiffness Control to the Benchmark Cable-stayed Bridge, *Journal of Structural Control*, *Special Issue on Cable-stayed Bridge Seismic Benchmark Control Problem*, Vol. 10, pp. 187-204, July-December, 2003.
9. Japan Roadway Association, *The Seismic Design Specification*, 1996.
10. Hanshin Highway Public Corporation, *Tempozan Bridge, Structure and Construction Data*, 1992. (in Japanese)
11. MathWorks, *MATLAB The Language of Technical Computing*. The MathWorks Inc., 2000.
12. Chopra, A. K., *Dynamics of Structures, Theory and Applications to Earthquake Engineering*, Prentice Hall, 1995.